Dynamic control for synchronization of separated cortical areas through thalamic relay.

Leonardo L. Gollo, Claudio R. Mirasso, Alessandro E.P. Villa

Dynamic control for synchronization of separated cortical areas through thalamic relay

Leonardo L. Gollo [a], Claudio Mirasso [a,*], Alessandro E. P. Villa [b]

[a] *IFISC, Instituto de Física Interdisciplinar y Sistemas Complejos (CSIC-UIB), Campus Universitat des Illes Balears, E-07122 Palma de Mallorca, Spain*

[b] *NeuroHeuristic Research Group*
http://www.neuroheuristic.org
Grenoble Institut des Neurosciences (GIN) UMR_S 836 INSERM, Université Joseph Fourier, Grenoble, France
and
Information Systems Department ISI, University of Lausanne, Switzerland

Abstract

Binding of features and information which are processed at different cortical areas is generally supposed to be achieved by synchrony despite the non-negligible delays between the cortical areas. In this work we study the dynamics and synchronization properties of a simplified model of the thalamocortical circuit where different cortical areas are interconnected with a certain delay, that is longer than the internal time scale of the neurons. Using this simple model we find that the thalamus could serve as a central subcortical area that is able to generate zero-lag synchrony between distant cortical areas by means of dynamical relaying (Vicente et al., 2008). Our results show that the model circuit is able to generate fast oscillations in frequency ranges like beta and gamma bands triggered by an external input to the thalamus formed by independent Poisson trains. We propose a control mechanism to turn "On" and "Off" the synchronization between cortical areas as a function of the relative rate of the external input fed into dorsal and ventral thalamic neuronal populations. The current results emphasize the hypothesis that the thalamus could control the dynamics of the thalamocortical functional networks enabling two separated cortical areas to be either synchronized (at zero-lag) or unsynchronized. This control may happen at a fast time scale, in agreement with experimental data, and without any need of plasticity or adaptation mechanisms which typically require longer time scales.

Key words: dynamic relaying, thalamocortical circuit, zero-lag synchronization, correlation, firing pattern, thalamus, reticular thalamic nucleus.

Introduction

In the central nervous system (CNS) it is assumed that the information is mainly represented by the activity of neurons transmitted to other neurons through synaptic links. The extent of the neural network activated by a specific "piece of information" is a never ending matter of investigation but it is accepted that both average levels of discharges, firing rate (Gollo et al., 2009), and precise spike timing contribute to neural coding. Spatiotemporal firing patterns (Villa et al., 1999b; Hayon et al., 2005) and coherent oscillatory neural activity (Fries et al., 2007) associated to sensory and behavioral events support the hypothesis that temporal information plays a key role in brain processing. Empirical phenomena and extensive experimental data validated across different species (Gray et al., 1989; Engel et al., 1991; Castelo-Branco et al., 2000; Tiesinga et al., 2008) emphasize the importance of emerging cortico-cortical synchrony as a major phenomenon for binding features distributed neural activity (von der Marlsburg, 1973; Fries, 2005; Desbordes et al., 2008). Despite the success of physical models to reproduce oscillatory patterns of neural activity it is not clear whether the synchronization is the result of network processing exclusively limited to cortico-cortical interactions or subcortical structures might also intervene (Contreras et al., 1996; Traub et al., 1996; Vicente et al., 2008; Chawla et al., 2001), for a recent review please refer to Uhlhaas et al. (2009).

The thalamus is a structure of CNS that could play an important role to let the emergence or to control cortico-cortical synchronization because the exchange of information between the thalamus and cerebral cortex is a general feature of all ascending sensory pathways but olfaction (Jones, 1985; Sherman, 2005). The connectivity pattern between thalamus and cortex is usually viewed as been characterized by thalamocortical integration and corticothalamic feedback (Steriade and Llinas, 1988; Villa et al., 1999a; Villa, 2002). Multiple thalamocortical modules characterized by the same basic connectivity may be assumed to work in parallel and include three main components (see Fig. 1): (i) dorsal thalamic neurons (e.g. from the medial geniculate body for the auditory pathway or from the lateral geniculate body for the visual pathway) recipient of the sensory input from the periphery; (ii) cells of the thalamic reticular nucleus (R), a major component of the ventral thalamus;

* Corresponding author.
Email addresses: leonardo@ifisc.uib.es (Leonardo L. Gollo), claudio@ifisc.uib-csic.es (Claudio Mirasso), avilla@neuroheuristic.org (Alessandro E. P. Villa).

(iii) the cortical area receiving the corresponding thalamic input. The thalamic reticular nucleus receives collateral inputs from both thalamocortical and corticothalamic fibres and sends its inhibitory projections to the dorsal thalamus, thus regulating the firing mode of the thalamocortical neurons. The thalamic reticular nucleus receives inputs also from several forebrain and midbrain areas known to exert modulatory functions (McCormick and Bal, 1994), in particular from nerve growth factor responsive basal forebrain cholinergic cells (Villa et al., 1996) that are involved in many cognitive functions and whose dysfunction is associated to Alzheimer's Disease. In the auditory system evidence exist that corticofugal activity regulates the response properties of thalamic cell assemblies by changing their bandwidth responsiveness to pure tones (Villa et al., 1991) thus allowing to selectively extract information from the incoming sensory signals according to the cortical activity (Villa et al., 1999a). This model suggests that the thalamocortical circuit carries embedded features that enable the build-up of combined supervised and unsupervised information processing akin to produce an adaptive filter (Tetko and Villa, 1997) aimed to select behaviorally relevant information processing (von Kriegstein et al., 2008).

The current study is not aimed at simulating any detailed thalamocortical circuit, but rather to assess the role of simple variables that could play a major role in controlling the emergence and maintenance of synchronized activity in distributed cortical areas that project to the same thalamic nuclei. Our model predicts that small changes in the cortical neurons firing rate, due to non-correlated background synaptic activity in the thalamic region, is capable of generating single or multi-frequency oscillations along with zero-lag synchronization between distant cortical regions. We quantify this synchronized state by measuring the signal-to-noise ratio which does not monotonically increase with the firing rate. According to our model, thalamic activity plays a key role in controlling the appearance of lag free synchronization between cortical areas. In addition, despite its simplification, the model provides hints about the conditions necessary to achieve that synchronization. We report an efficient control set as the ratio of dorsal over ventral thalamus external input activity to switch on thalamocortical synchronous dynamics. That switch occurs at a fast time scale, without any need of synaptic plasticity which would require longer time scales (Fries, 2005). The type of control that we suggest is not limited to an "On"-"Off" switch, but it allows to control the appearance of synchronous activity over an extended range of frequencies despite the delays involved in the long-range cortico-cortical interactions (Ringo et al., 1994; Vicente et al., 2009).

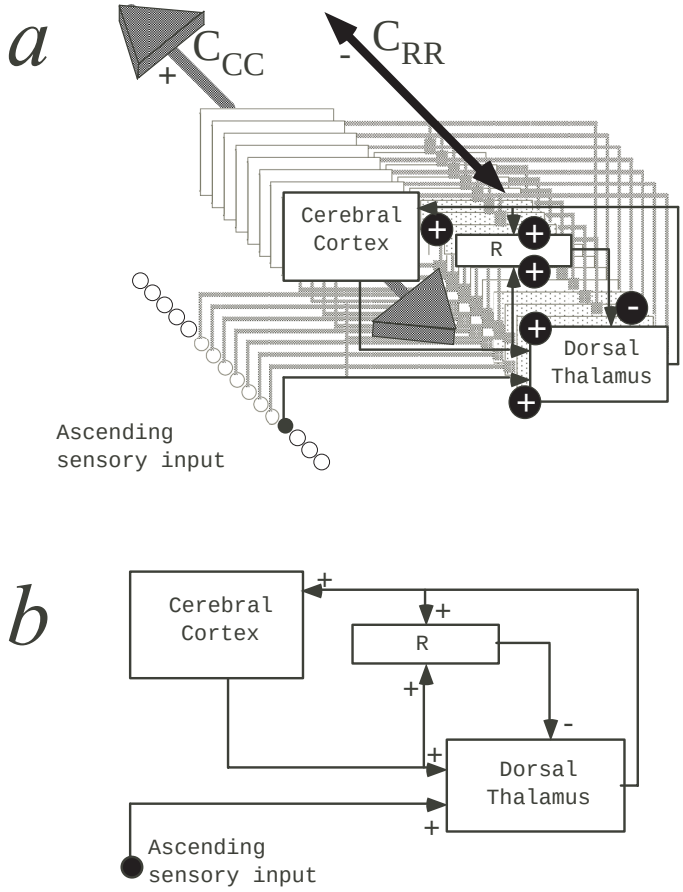

Fig. 1. **(a)** A functional scheme of the modular organisation of the typical thalamocortical sensory pathway (somatosensory, visual, sensory). The signs indicate the nature of the connections, (+) excitatory and (-) inhibitory. Notice the big arrows labeled C_{CC} corresponding to long-range excitatory cortico-cortical connections and C_{RR} corresponding to the inhibitory connections within the reticular and perigeniculate nucleus of the thalamus (R). Note the excitatory input from the ascending sensory pathway to the dorsal thalamus, the excitatory projection from the thalamus to the cortex with a collateral to R, and the excitatory projection of the cortex to the thalamus with a collateral to R. The only output of R is an inhibitory backprojection to the thalamus. **(b)** Explicit connections within one thalamocortical module.

Methods

To study the synchronization of cortical activity facilitated by the thalamic relay we conducted extensive numerical simulations of a reduced thalamocortical model of spiking integrate–and–fire neurons subject to background noise and an external driving. The model includes both local synapses and long-range interactions with different delays according to functional connectivity in a four populations motif (Milo et al., 2002) (Fig.2). The simulations were performed using NEST, the neuronal simulation tool (Brette et al., 2007) with

the PyNEST interface (Eppler et al., 2009).

Neuronal model. The integrate-and-fire neuron model (Brunel, 2000) for each neuron i satisfies the following dynamical equation for the membrane potential $V_i(t)$:

$$\tau_{mem}(m)\frac{dV_i(t)}{dt} = -V_i(t) + RI_i(t) \ , \tag{1}$$

where $\tau_{mem}(m)$ is the membrane time constant of neuron i belonging to the population m (as in Fig. 2); $I_i(t)$ is the total current arriving to the soma. The last term in the above equation is given by the sum of all postsynaptic potentials (PSP) of neurons belonging to the network plus the total postsynaptic potentials of all external neurons, the latter being modeled as a Poisson process. Thus,

$$RI_i(t) = \tau_{mem}(m) \sum_j J(j) \sum_k \delta(t - t_j^k - \tau(z,m)) + V_{ext} \ . \tag{2}$$

The first sum is taken over all presynaptic neurons j, each neuron receives $C_e(m,z)$ excitatory synapses and $C_i(m,z)$ inhibitory synapses and they depend on the inter-population (long-range) connections z if both neurons belong to different populations or otherwise on the population m to whom they belong. t_j^k is the time of the $k-th$ spike received by neuron i from its neighbor j. The axonal conduction delay is given by $\tau(z,m)$, which corresponds to a spike of a presynaptic neuron j that reaches neuron i. $J(j)$ stands for the PSP and depends on whether its presynaptic neighbor neuron j is excitatory ($J(j) = J_e$) or inhibitory ($J(j) = J_i$). V_{ext} is the postsynaptic potential generated by neurons from outside the thalamocortical network. It is given by an independent and homogeneous Poisson process of N_{ext} external neurons, each one firing with a fixed average rate $\nu(m)$. The external spike contributes with a change of the membrane potential by J_{ext} whenever it impinges upon neuron i. The dynamics of the neurons can be described as following: the neurons start at a rest potential $V_r(m)$ which can be changed by the synaptic current. If the potential $V_i(t)$ of the i-th neuron reaches the threshold $\theta(m)$ a spike is generated and its membrane potential is reset to $V_r(m)$ after an absolute refractory period ($\tau_{rp} = 2\ ms$).

After a brief parameter search and according to the range of values described in the literature we have set characteristic parameters for each population m presented in Table 1. The rational of our choice was to preserve the simplicity of an oversimplified model of the thalamocortical circuit, though retaining the main dynamical features. The values of the threshold, the resting membrane

potential, and the membrane time constants were selected such that the neurons in R were the most excitable and those in T were the least excitable because T neurons are meant to receive the external input arising from the ascending sensory pathways. For the sake of simplicity, the refractory period and the excitatory/inhibitory postsynaptic efficacies were chosen to be the same for all neurons.

Table 1
Neuronal parameters for the neurons in population m. *Each neuron receives also afferences from a random neuron of the same population.

population (m)			Parameter	
C_1, C_2	R	T		
800	0	200	$N_e(m)$	# of excitatory neurons
200	40	0	$N_i(m)$	# of inhibitory neurons
20	25	15	$\tau_{mem}(m)$	membrane time constant (ms)
20.5	24.65	15	$\theta(m)$	threshold value (mV)
2	2	2	τ_{rp}	refractory period (ms)
10	12.5	7.5	$V_r(m)$	membrane rest potential (mV)
80	0	5	$C_e(m)$	# of excitatory synapses*
20	10	0	$C_i(m)$	# of inhibitory synapses*
1.5	2	1	$\tau(m)$	synaptic delay (ms)
0.05	0	0.05	J_e	excitatory postsynaptic efficacy (mV)
-0.2	-0.2	0	J_i	inhibitory postsynaptic efficacy (mV)

Thalamocortical model. The topology of the model is characterized by two thalamic and two cortical neural populations (Shepherd, 1998; Huguenard and McCormick, 2007). The overall layout of our model is depicted in Fig. 2. The thalamus is composed by two separate populations, one of excitatory thalamocortical principal cells (T) and another of inhibitory neurons corresponding to the thalamic reticular and perigeniculate nuclei (R). The two thalamic populations are also characterized by recurrent intrathalamic connections. The cortical populations are formed by an excitatory cell type with local, long range cortical, and feedback corticothalamic projections and by an inhibitory type characterized by only local efferent projections. In addition, the two cortical populations are distributed in two "areas" (C_1 and C_2) which may or may not be interconnected (following the value of parameter C_{CC}). It is a hierarchical network, with both an intra-population random structure and a simple inter-population pattern of connectivity with longer delays. The populations have both internal and external connectivity. Then, the topology

satisfies the following constrains: both R (C_{CR}) and T (C_{CT}) populations receive cortical feedback, the cortical populations are innervated by T (C_{TC}) but do not receive inhibitory feedback from R. There are also direct connections from R to T (C_{RT}) and from T to R (C_{TR}). Long range cortico-cortical connections are determined by C_{CC}. Assuming that the thalamus is composed by both R and T populations, the thalamocortical model may also be reduced to a three populations network formed by a central thalamic region (T and R) and two balanced cortical areas. Each neuron of a given population receives the same amount of postsynaptic connections. The presynaptic neurons are set randomly, therefore, the postsynaptic distribution is binomial for each type of neuron (excitatory or inhibitory) within a given population.

Table 2
Parameters for inter-population (long-range) connections z between any two regions. Each neuron of the target population receives input from a randomly selected neuron belonging to the efferent population.

inter-population connectivity (z)						Parameter	
CR	CT	TC	RT	TR	CC		
30	20	20	0	80	0-110	$C_e(z)$	# of excitatory synapses*
0	0	0	25	0	0	$C_i(z)$	# of inhibitory synapses*
8	8	5	2	2	5	$\tau(z)$	synaptic delay (ms)

The connectivity parameter values described in Table 2 were set arbitrarily in order to maintain the relative proportion of cell types usually described in the literature (Jones, 1985; Sherman, 2005). The number of connections were set to keep 160 afferences to each neuron of C, 75 afferences to each neuron of T and 150 afferences to each neuron of R. This pattern of convergence-divergence is meant to preserve the known anatomical thalamocortical and corticothalamic pattern of connectivity (Jones, 1985; Sherman, 2005). The specific proportion of afferences generated by each population is indicated in the boxes at the bottom of Fig. 2. The delays were set to account for typical axonal delays described in the thalamus and cortex of mammals (Swadlow, 2000; Knoblauch and Sommer, 2004). Despite the fact that we have not systematically investigated all ranges of axonal delays, we observed that the results are robust against these delays. The most critical parameter is the delay between the thalamus and the cortical areas (τ_{TC}) which must be kept identical for all ascending projections. If this delay is not the same for all TC connections the maximum number of coincident spikes in the cross-correlograms does not occur at zero-lag but at a lag that depends on the difference between the TC time delays. It is worth mentioning that a constant latency between thalamus and cortex irrespective of the distances has been reported due to regional myelination differences that compensate for the conduction velocities (Salami et al., 2003).

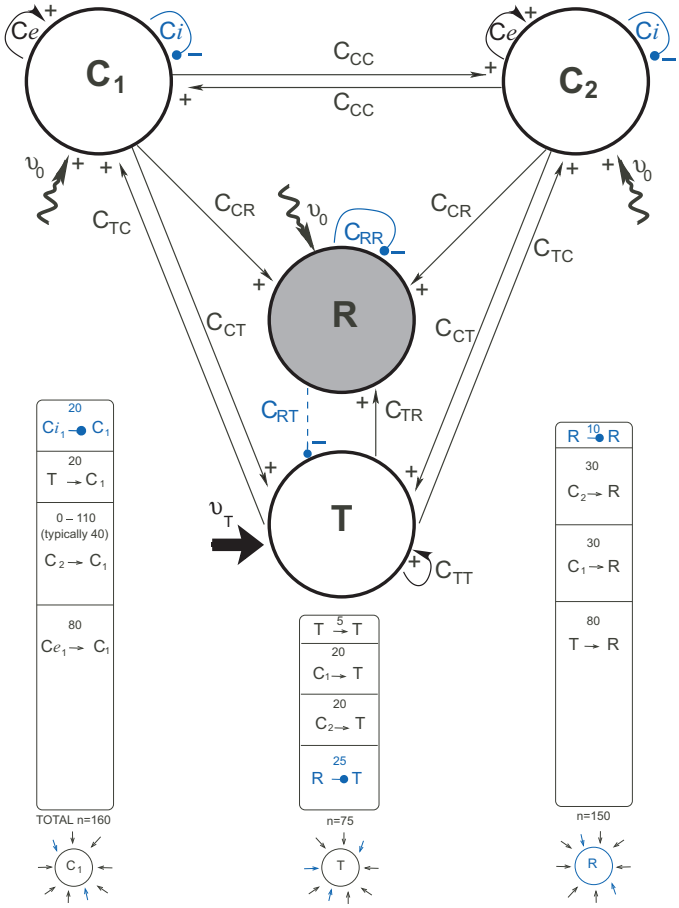

Fig. 2. Circuit layout. The sign at the arrow tip indicate the effect of the connection either excitatory (+) or inhibitory (+). Notice that the inhibitory projections are represented with a rounded shape tip. The boxes at the bottom of the figure show the pattern of the afferences of a cortical area (C_1, bottom left), of principal thalamic neurons (T, bottom centre), and of thalamic reticular neurons (R, bottom right). The thalamus is formed by two neuronal populations, the excitatory thalamocortical projecting neurons (T) and the inhibitory reticular and perigeniculate neurons (R) which are reciprocally interconnected (C_{TR},C_{RT}). In addition, there are local excitatory connections (C_{TT}) between thalamic principal cells and local inhibitory connections (C_{RR}) between reticular thalamic cells. Two cortical "areas" (C_1 and C_2) are connected to the same thalamic region. Each cortical area includes both excitatory (80%) and inhibitory (20%) neurons. The cortical excitatory neurons send feedback projections to the thalamus (C_{CT},C_{CR}), and establish long range corticocortical projections (C_{CC}) and local connections (Ce). The cortical inhibitory neurons establish only local connections (Ci). The inter-population connectivity is described by the parameters of Table 2. The background activity at rate ν_0 and the external input at rate ν_T consist of independent Poisson trains with parameters of Table 3. Neurons in T are the only ones receiving an external input meanwhile all other neurons receive background activity. The external input is uncorrelated and defines the key parameter: $\frac{\nu_T}{\nu_0}$.

Table 3
Parameters of the background and external afferences.

0.1 mV	J_{ext}	external synaptic efficacy
10.0 Hz	ν_0	external driving Poisson mean rate to C and R
8.0-45.0 Hz	ν_T	overall external driving Poisson process to T
450	N_{ext}	number of external afferences

Background activity and external input. To model the background activity we assume that each neuron in the network is connected with N_{ext} excitatory external neurons subject to an independent random Poisson processes with average rate ν_0 for neurons of all regions. The thalamic region (T) receives the background activity combined with an external input also modeled by independent Poisson process, such that both the overall external input to T is a process characterized by rate ν_T. The parameters used for the Poisson background and the external driving are presented in Table 3.

Cross-correlation analysis. We run extensive simulations and analyze the spike trains over several trials. In order to quantify the results from the numerical simulations, we define two values from the cross-correlogram: a) its mean value representing the "noise" level quantifying the expected number of coincidences by chance; b) the peak of the cortico-cortical cross-correlogram (typically at zero-lag) that stands for the "signal". Those quantities are used to compute the signal-to-noise ratio for different values of ν_T and different strengths of cortical interconnectivity (C_{CC}). The results are averaged over 100 trials during $2,000\ ms$ in a stationary regime after $500\ ms$ of transient dynamics. The averaged result is condensed in a single cross-correlogram, which measures the mean number of coincidences (in a $2\ ms$ bin) of $3,000$ randomly selected neuron pairs belonging to different populations and also averaged over the trials. This procedure allows us to assess the mean behavior of the dynamics and eliminate single trial fluctuations.

The "noise" is determined by the mean over the time lag in the averaged cross-correlogram. It can also be calculated analytically considering the activity of the two populations just as been independent: Let $F(p)$ be the mean firing rate of a population p and b the bin size of the computed cross-correlogram, therefore the mean cross-correlogram (noise) of two arbitrary populations i and j is given by $\langle XCOR_{i-j} \rangle = F(i)F(j)b$. For a typical thalamocortical circuit the two cortical areas have either maximum synchrony at zero-lag or no synchrony (unless C_{CC} is greater than the number of internal excitatory cortical connections C_{eC}). Thus the "signal" of the cortico-cortical dynamics is defined as the number of coincidences in the cross-correlogram at zero time lag.

Results

We have simulated the activity of large populations of interacting neurons with delayed connections. We used a simple integrate and fire (I&F) neuronal model in order to keep the problem easily computationally tractable. The model retains threshold dynamics and if the membrane potential reaches the threshold a spike is fired. The membrane potential is reset after the firing to its resting potential with an absolute refractory period (2 ms). The spike is transmitted to all target neurons which receive an excitatory or inhibitory postsynaptic potential according to the type of synapse. The spike is transmitted with a delay depending on the connection type. Large delays are associated with inter-population connections and short delays with local connections within each population. The results analyze the firing rate, cross-correlation indicators, oscillation and synchronization information calculated from the spike trains of individual neurons and neuron populations. It is worth mentioning that the neuronal spike times were reliably reproduced despite the simplicity of the I&F model.

Thalamocortical circuit dynamics. In the most symmetrical case, the T region is set in order to receive external driving with the same rate as the other populations ($\nu_T = \nu_0$). The firing rate in R is higher than in the cortex which is also higher than in T. For a typical number of cortico-cortical interaction, say $C_{CC} < 40$, due to the network connectivity and the difference in the neuronal parameters, there is no correlation among the different areas, and the activity is random and irregular. For $\nu_T > \nu_0$ other scenario takes place. The raster plots of 150 neurons randomly chosen among all neuronal populations illustrate the network dynamics. Such a typical raster plot is depicted in Fig. 3a. It shows the case in which the cortico-cortical connections are set as $C_{CC} = 40$ and the thalamus is receiving an external input of mean rate $\nu_T = 7/3\nu_0$. The neurons within the populations T and R are synchronized at a high frequency. The two cortical areas exhibit a large number of coincidences at zero-lag, meaning that they are synchronized and *in-phase*. The cross-correlograms (see Methods section for details) between the cortical areas and between the thalamus and one cortical area are shown in Fig. 3b,c. The graphic clearly indicates *in-phase* correlation among cortical areas while the thalamus and the cortical area are out of phase (with the cortical area delayed by 6 ms).

The synchronization of the cortical regions depends on the external input to T. Fig. 4 shows the raster plot of a single trial characterized at $t = 50$ ms by a sudden increase of the T activity from the mean rate ν_0 to $7/3\nu_0$. The synchrony does not occur in the system for low values of input ν_T, for instance $\nu_T = \nu_0$, from 0 ms to 50 ms or after the input is switched off, say for time

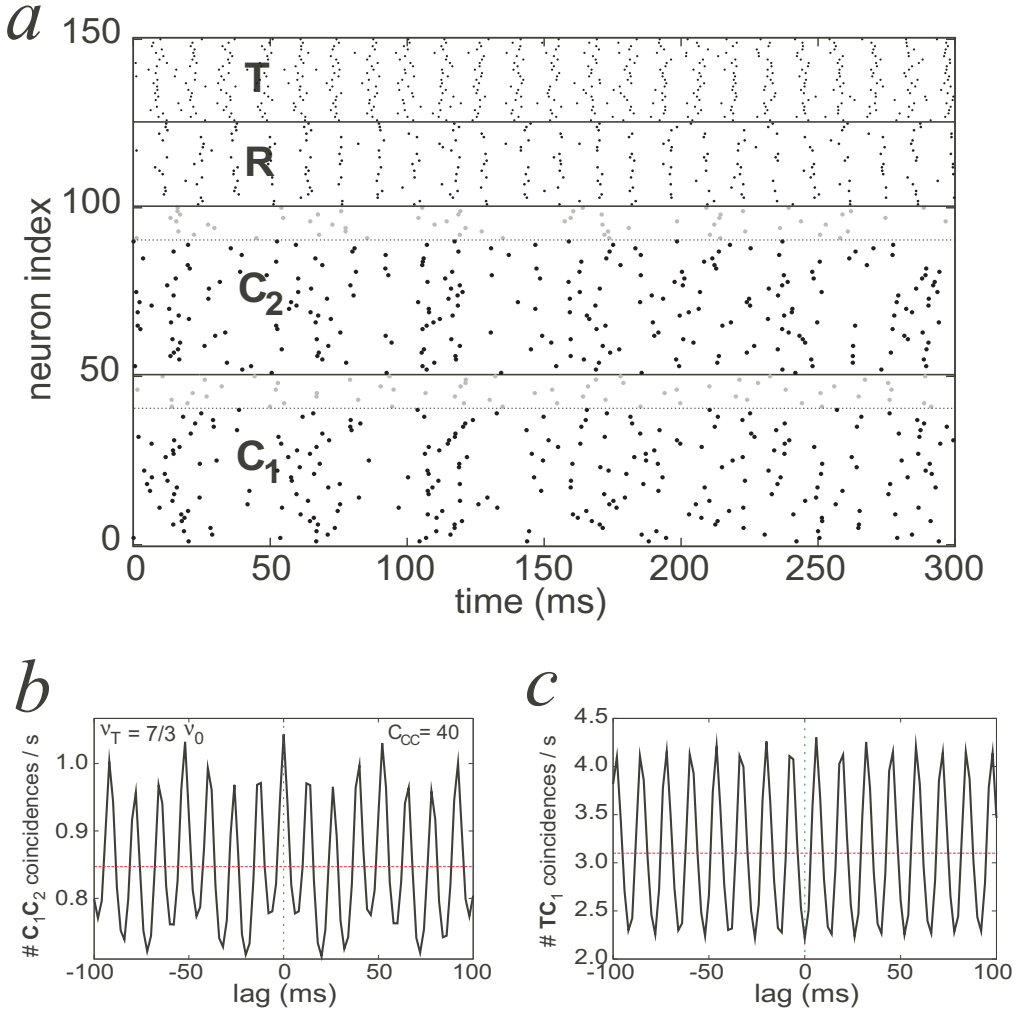

Fig. 3. Thalamocortical dynamics. **(a)** Raster plots of 150 neurons randomly chosen (50 from each cortical population and 25 neurons from R and T). The firing times of the local cortical inhibitory neurons are represented by grey dots. R, C_1, C_2 receive a background Poissonian noise at rate ν_0 Hz. T receives a Poissonian noise at rate $\nu_T = \frac{7}{3}\,\nu_0$. **(b)** Averaged cross-correlogram of 3,000 randomly selected neuronal pairs of different C_1 and C_2 populations averaged over 100 trials. Bin size 2 ms. The horizontal line correspondings to the mean value stands for the *noise*. The peak at zero-lag stands for the *signal*. These values are used to compute the *signal-to-noise* ratio (see text for details). **(c)** Averaged cross-correlogram of 3,000 randomly selected neuronal pairs of different T and C_1 populations averaged over 100 trials. Same labels as panel (b). Notice that the maximun of C_1-C_2 crosscorrelation occurs exactly at zero-time lag while the maximum of T-C_1 occurs at a lag of 6 ms.

$t > 250$ ms.

The mean firing rate of T, C, and R neurons, computed over $2,000$ ms, increases monotonically as a function input rate ν_T (Fig. 5a). The dependency

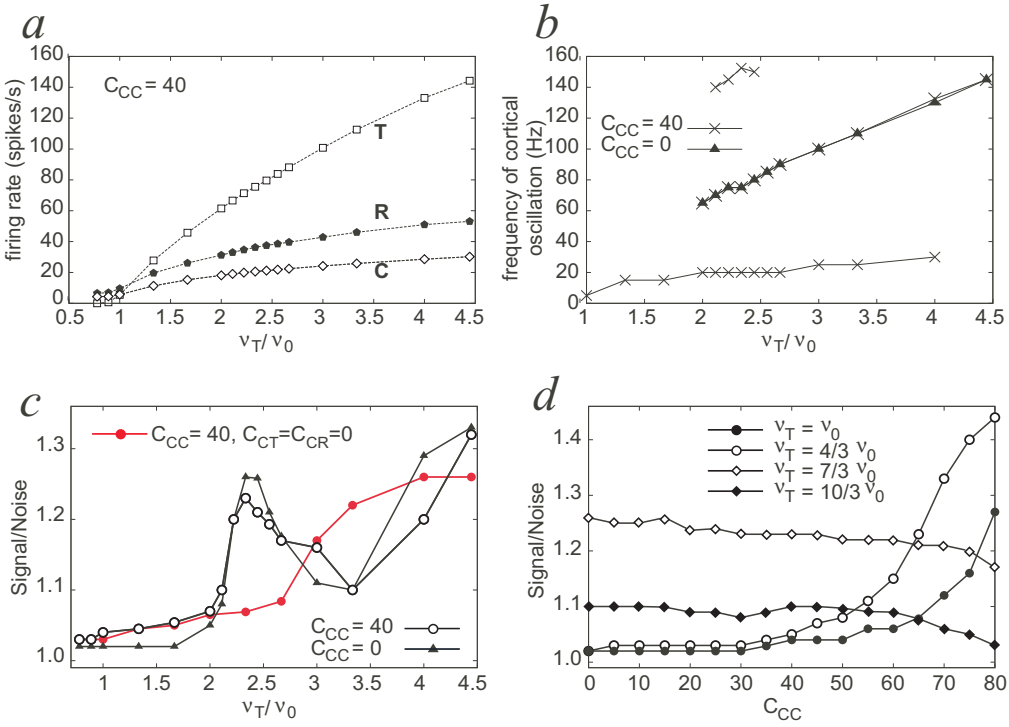

Fig. 5. Unveiling the dynamics - 100 trials analysis. **(a)** Diagram of the mean firing rate of T (open squares), R (bold dots) and C (open diamonds), as a function of the external input ν_T. **(b)** Diagram of the frequencies of cortical oscillations for increasing ν_T. The frequencies correspond to the peaks of the spectrum calculated from the Fourier transform of the cross-correlograms. Crosses indicate the data calculated with coupled cortical areas ($C_{CC} = 40$) and solid triangles were calculated in the absence of cortico-cortical coupling ($C_{CC} = 0$). **(c)** Signal-to-noise ratio as a function of the external input ν_T. Cortico-cortical coupling was set to zero (open dots) and $C_{CC} = 40$ (solid traingles). A special case with no corticofugal connectivity ($C_{CR} = C_{CT} = 0$) is plotted (solid dots) for comparison. **(d)** Signal-to-noise ratio as a function of the strength of cortico-cortical connectivity. We compare the curves for different values of ν_T.

of the cortical oscillation frequency as a function of ν_T/ν_0 is shown in Fig. 5b for directly interconnected ($C_{CC} = 40$) and disconnected ($C_{CC} = 0$) cortical areas. The frequencies are determined from the power spectrum analysis of the cross correlograms. Only those components whose power is larger than 20% of the maximum power are considered here. In the disconnected case, the cortical areas oscillate at a single frequency close to the thalamic firing rate (see rate in Fig. 5a). In the interconnected case ($C_{CC} = 40$) a single frequency dominates the oscillatory dynamics only if $\nu_T < 2\nu_0$. Beyond this threshold at least two frequencies of oscillation appear. For $\nu_T = \frac{7}{3}\nu_0$ three different frequencies are observed (as in Fig. 3b). The lowest frequency is related to the firing rate of the neurons within the cortical areas. The intermediate frequency is related to the thalamic firing rate like in the disconnected case. An increase of the oscillatory frequency in the cortical areas is due to greater interaction between

the cortex and the thalamus as a function of a larger input fed into the thalamus. The highest frequency component in the interconnected case ($C_{CC} = 40$) is likely to be related to the inverse of the delay time of the cortico-cortical connection. However, this frequency component is observed only for a very small range of input values.

The signal-to-noise ratio, as defined in the Methods section from the cross-correlograms, as a function of ν_T/ν_0 is illustrated in Fig. 5c. The firing rate and the "signal" increase monotonically with the external rate of the input, but interestingly SNR is characterized by a local maximum for uncoupled cortical areas as well as for coupled cortico-cortical areas with connectivity $C_{CC} = 40$. The signal-to-noise was quite flat for low values of ν_T, then increases until reaching the local maximum. After decreasing from the local maximum the signal-to-noise increases again monotonically for very large values of the rate ν_T. To gain insight whether the synchronization among the cortical areas is induced by the T-R circuit into this aspect, we allowed the system to evolve with the whole connectivity and suddenly cut the cortico-thalamic connections ($C_{CR} = C_{CT} = 0$). The results are shown with solid dots in Fig. 5c. This curve shows that for $2 < \nu/\nu_0 < 3$ the SNR is much smaller than the one obtained with the whole connectivity, indicating that the synchronization is not driven by the thalamus circuit. Instead, a true collective behavior emerges from the whole interaction. For $\nu/\nu_0 \sim 3$ the curve increases suddenly, thus indicating that the synchronization starts to be driven by the activity of the thalamus. The signal-to-noise ratio as a function of the strength of the cortico-cortical connection for different values of ν_T/ν_0 is illustrated in Fig. 5d. Interestingly, for low values of ν_T/ν_0 the signal-to-noise response is flat but increases for large C_{CC} while it is flat but decreases for higher values of ν_T/ν_0.

Effect of the cortico-cortical connection. The mean firing rate F of the three neuronal populations as a function of the strength C_{CC} at an input level $\nu_T = 7/3\nu_0$ is illustrated in Fig. 6a. This figure shows that the cortical firing rate is indeed the most affected rate and increases monotonically with an increase in the cortico-cortical connectivity. The dominant frequencies of cortical oscillations determined by the power spectrum analysis are displayed in Fig. 6b as a function of cortical connectivity and for two levels of external input to the thalamus. For a value $\nu_T = 5/3\nu_0$ a single frequency appears almost constant and independent of the C_{CC} strength. On the contrary, at $\nu_T = 7/3\nu_0$ three frequency components appear for $C_{CC} > 35$. Like in Fig 5b the lowest frequency is associated to the cortical firing rate and the intermediate frequency is associated to the firing rate of population T. The highest frequency could also be associated to the inverse of the delay time in the cortico-cortical connection and became more important for higher values of C_{CC}. The presence of multiple oscillatory frequencies can be clearly observed in the cross-correlogram for $C_{CC} = 60$ and $\nu_T = 7/3\nu_0$ (Fig. 6c), whereas a

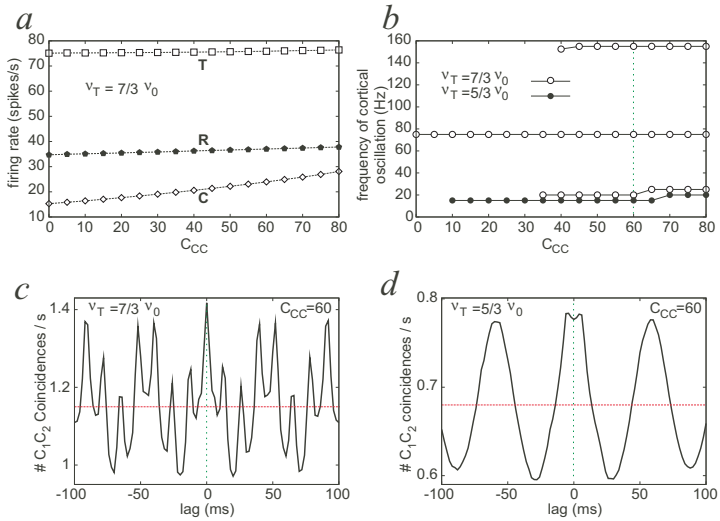

Fig. 6. Effect of the cortico-cortical connectivity. **(a)** The firing rate of T, R and C as a function of the cortico-cortical strength for $\nu_T = 7/3\nu_0$. **(b)** Frequencies of cortical oscillations for increasing values of C_{CC} for two different values of ν_T ($5/3\nu_0$; $7/3\nu_0$). **(c)** Cross-correlogram between C_1 and C_2 for $C_{CC} = 60$ and $\nu_T = 7/3\nu_0$. Notice the local maxima next to zero-lag are located at ± 12 ms. **(d)** Same as panel (c) but for $\nu_T = 5/3\nu_0$. Notice that the maxima are not exactly at zero-lag but at ± 6 ms.

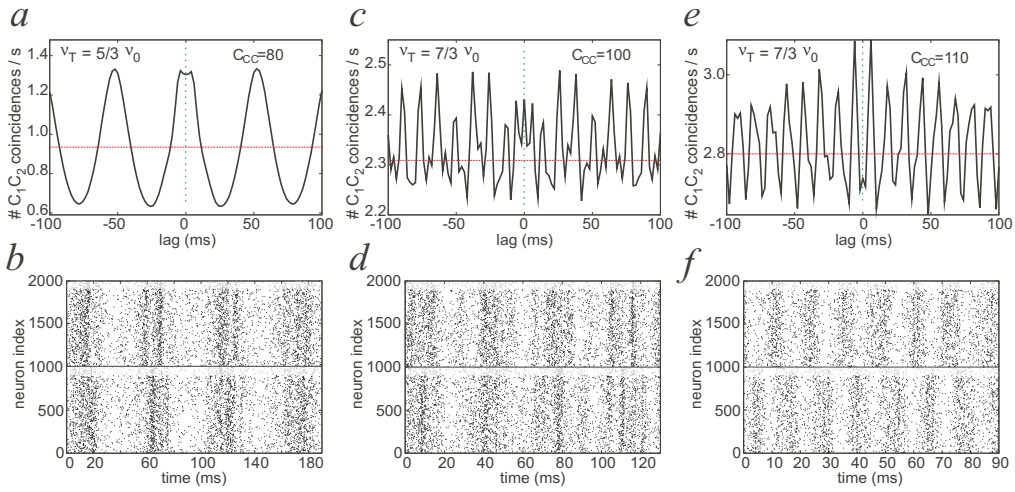

Fig. 7. Dynamics of the cortical area as a function of the cortico-cortical interaction strength. **(a,b)** The uper panel shows the cross-correlogram for $\nu_T = 5/3\nu_0$ and $c_{cc} = 80$. The lower panel shows the corresponding raster plot for all cortical neurons. C_1 neurons are indexed from 1 to 1000 and C_2 neurons are indexed from 1001 to 2000. **(c,d)** Same as previous for $\nu_T = 7/3\nu_0$ and $c_{cc} = 100$. **(e)** Same as previous for $\nu_T = 7/3\nu_0$ and $c_{cc} = 110$.

single frequency component dominates the dynamics for $\nu_T = 5/3\nu_0$ (Fig. 6d).

The observation of the raster plots and of the cross-correlograms illustrates further the dynamics emerging from the interaction between the cortical areas. In Fig. 7a, b it can be observed that for $C_{CC} = 60$ and $\nu_T = 5/3\nu_0$ the slow frequency component related to the cortical firing frequency is predominant. The peak is not sharp, at ± 4 ms from the zero-lag, and a "master-slave" dynamics can be observed in the region of high instantaneous firing rate (say from 50–80 ms after the external input onset). With parameters of $C_{CC} = 100$ and $\nu_T = 7/3\nu_0$ multiple frequencies are observed in the raster plot and in the cross-correlogram (Fig. 7c,d). In this case, both the zero-lag cortical synchronization and the leader-ladder dynamics present a strong competition. At very large values $C_{CC} = 110$ the cortico-cortical connection dominates and gives rise to an out-of-phase cortical synchronized dynamics between the two areas (Fig. 7e,f) The signature of this dynamics appears both in a double peak at $\pm$6ms (corresponding to the cortico-cortical coupling time in the cross correlation function) and in the raster plot where zero-phase synchronization does not occur between the cortical areas.

Discussion

We have presented the dynamics of a simplified thalamocortical circuit. Our results suggest that the thalamus could be a central subcortical area that is able to trigger the emergence of zero-lag synchrony between distant cortical areas due to a dynamical relaying (Fischer et al., 2006; Vicente et al., 2008). According to this phenomenon a central element can enable two populations to synchronize at zero-lag. Other subcortical areas such as the brainstem (Scheller et al., 2009) and the hippocampus are likely to play a similar role in dynamical relaying. However, the peculiar recurrent connections of the thalamic reticular nucleus (Jones, 1985; Sherman, 2005) might provide the thalamocortical circuit with specific features that do not account just for the synchronized pattern, but also for switching "on" or "off" the asynchronous state. Furthermore, considering that large scale integration may occur as a consequence of neuronal coherence, the critical question about how the dynamical selection of integrated areas is achieved remains open (Salinas and Sejnowski, 2001; Fries, 2005; Vicente et al., 2008; Uhlhaas et al., 2009). We suggest that an increase in the external activity fed into the T population with respect to that of R yields the cortical areas synchronize at zero-phase lag as depicted in Fig 3. That means the thalamus would be able to control the cortical synchronous state and regulate large scale integration. This control can occur at a fast time scale in agreement with experimental data and without any need of plasticity or adaptation mechanisms which typically require longer time scales. The main input sources to T are the ascending sensory input and the descending cortico-fugal pathway, thus suggesting that both inputs may play an important role in controlling cortical synchrony. This hypothesis for the cortico-petal projections is complementary to the hypothesis of "adaptive filtering" suggested elsewhere for the cortico-fugal projections (Villa et al., 1991, 1999a; Tetko and Villa, 1997).

According to our model, see Figs. 5b, 6b, the thalamocortical circuit is able to generate fast oscillations in frequency ranges like beta and gamma bands triggered by an external input to the thalamus formed by independent Poisson trains. The question of how to generate such fast oscillations has been largely discussed in the literature (Traub et al., 1996; Doiron et al., 2003; Doiron et al., 2004; Börgers et al., 2005; Marinazzo et al., 2007; Börgers et al., 2008) but, as recently pointed out (Nikolić, 2009), empirical phenomena like the cycle skipping were not satisfactorily described. The cycle skipping is observed experimentally in the current thalamocortical model when each cortical neuron spikes according to a gamma frequency modulation but with a smaller firing rate. In the raster plots of Fig. 3a it is possible to observe that few neurons spike at a given gamma cycle. Then, the oscillations are in fact shared by a whole population while single neurons skip cycles. As shown in Figs. 5a, b the cortical oscillations, for instance at a signal-to-noise ratio local maximun $\nu_T \simeq$

$\frac{7}{3}\ \nu_0$, occur at frequencies near 80 Hz for disconnected areas and in multiple frequencies for $C_{CC} = 40$, while the average firing rate is approximately $\frac{1}{4}$ of it, 20 $spikes/s$. In general, the firing rate of the cortical populations (see Figs. 5a, 6a) were found to be related to the lowest frequency component in case of multiple frequency oscillations. Otherwise the cortical firing rate tends to be much lower than the single frequency of oscillations (e.g., Fig. 5b) or close to it for low external driving ($\nu_T = \frac{5}{3}\ \nu_0$), e.g., Fig. 6b.

The current results emphasize the hypothesis that the thalamus could control the dynamics of the thalamocortical functional networks enabling two separated cortical areas to be either synchronized (at zero-lag) or unsynchronized. Correlations in the output firing rate of two neurons have been shown to increase with the firing rate (de la Rocha et al., 2007). Indeed we observed that for increasing input rates (ν_T) the firing rate of all populations increase monotonically, accordingly to an expected sigmoidal function (Fig. 5a). König and collaborators (König et al., 1995) reported physiological evidence of long-range synchrony with oscillations, whereas short-range synchrony may occur with or without oscillations. Our results, especially for low number of cortico-cortical inter-population synapses (say smaller than the internal connectivity), are in agreement with this finding. However, synchrony without oscillations in local circuit may appear due to extensive sharing of common excitatory inputs which typically generate the zero-lag coincidence observed when neurons are fire at high rates (de la Rocha et al., 2007). Conversely, neurons correlated by long-range connections are likely to share very few synaptic driving, such that synchrony without oscillations should be very rare.

In order to suggest an insight of the model with the anatomical pattern of the circuit one should consider that the thalamocortical and corticothalamic projections are reciprocal to a great extent but corticothalamic projections are characterized by a dual pattern of synapses on the thalamic neurons. Small endings formed the major corticothalamic terminal field, whereas giant terminals were less numerous and formed additional terminal fields together with small terminals. (Rouiller and Welker, 2000; Takayanagi and Ojima, 2006). The modal switch of corticothalamic giant synapses controlled by background activity was recently reported (Groh et al., 2008). We speculate that this finding and our results may suggest that each pattern of corticothalamic synapse might correspond to a different function. One synaptic type might be involved in assessing the circuitry necessary for the build-up of cortico-cortical synchronization. The other synaptic type would be involved in transmitting stimulus-related information. Which is which is a question that the current study is unable to answer. We must also consider the fact that our model of individual dynamics of the integrate-and-fire neurons does not produce burst discharges (Sherman, 2001; Krahe and Gabbiani, 2004). This is a clear limitation and the inclusion of a more physiologically realistic model as well as greater neuronal diversity (Buia and Tiesinga, 2008) are scheduled for our future work. Despite

the simplification of our circuitry and the neuronal network modeling in general the robustness of our model is an interesting outcome of this study. The zero-lag synchrony between the cortical areas depends only on the identical axonal delays $\tau(TC)$. If these delays are not the same for all TC connections the maximum number of coincident spikes in the cross-correlograms does not occur at zero-lag but at a lag that depends on the difference between the TC time delays. However, it is worth mentioning that regional myelination that compensates for changes in the conduction velocity has been reported as a mechanism that could keep constant latency between thalamus and cortex irrespective of the distances. Moreover, our results are in agreement with the suggestion reported by Chawla et al. (2001) about the key role of the thalamus favoring the zero-lag synchronization.

We have arbitrarily kept the external input ν_0 over R and the cortex populations fixed but we might have kept fixed T and the cortex populations with a variable external input into R (ν_R). In fact it is the dependency on the variable $\frac{\nu_T}{\nu_R}$ which represents the control key of the dynamic activity of the system as both rates of external inputs (ν_T, ν_R) are varying over time (McAlonan et al., 2008; Yu et al., 2009). The importance of uncorrelated inputs can be viewed as emphasizing the role of so-called "background activity", which was already reported to play an important role in controlling the thalamocortical circuit dynamic state (Wolfart et al., 2005). We are convinced that further simulations with more accurate details of the neuronal models and with embedded models of the dual cortico-fugal connectivity may provide critical clues for better understanding the mechanisms of the dynamical control subserving the synchronization of cortico-cortical distributed activity.

Acknowledgments

We thank Raul Vicente and Javier Iglesias for useful comments and suggestions. The authors acknowledge financial support from the European Commission Project GABA (FP6-NEST Contract 043309), LLG and CM also acknowledge the MEC (Spain) and Feder under project FIS2007-60327 (FISICOS).

References

Börgers, C., Epstein, S., Kopell, N. J., 2005. Background gamma rhythmicity and attention in cortical local circuits: A computational study. Proceedings of the National Academy of Sciences of the United States of America 102 (19), 7002–7007.

Börgers, C., Epstein, S., Kopell, N. J., 2008. Gamma oscillations mediate stimulus competition and attentional selection in a cortical network model. Proceedings of the National Academy of Sciences 105 (46), 18023–18028.

Brette, R., Rudolph, M., Carnevale, T., Hines, M., Beeman, D., Bower, J. M.,

Diesmann, M., Morrison, A., Goodman, P. H., Harris, Jr., F. C., Zirpe, M., Natschlager, T., Pecevski, D., Ermentrout, B., Djurfeldt, M., Lansner, A., Rochel, O., Vieville, T., Muller, E., Davison, A. P., El Boustani, S., Destexhe, A., 2007. Simulation of networks of spiking neurons: a review of tools and strategies. Journal of Computational Neuroscience 23, 349–398.

Brunel, N., 2000. Dynamics of sparsely connected networks of excitatory and inhibitory spiking neurons. Journal of Computational Neuroscience 8, 183–208.

Buia, C. I., Tiesinga, P. H., 2008. Role of Interneuron Diversity in the Cortical Microcircuit for Attention. J Neurophysiol 99 (5), 2158–2182.

Castelo-Branco, M., Goebel, R., Neuenschwander, S., Singer, W., 2000. Neuronal synchrona correlates with surface segregation rules. Nature 405, 685–689.

Chawla, D., Friston, K. J., Lumer, E. D., 2001. Zero-lag synchronous dynamics in triplets of interconnected cortical areas. Neural Networks 14 (6-7), 727 – 735.

Contreras, D., Destexhe, A., Sejnowski, T., Steriade, M., 1996. Control of spatiotemporal coherence of a thalamic oscillation by corticothalamic feedback. Science 274, 771–774.

de la Rocha, J., Doiron, B., Shea-Brown, E., Josic, K., Reyes, A., 2007. Correlation between neural spike trains increases with firing rate. Nature 448, 802–806.

Desbordes, G., Jin, J., Weng, C., Lesica, N. A., Stanley, G. B., Alonso, J.-M., 12 2008. Timing precision in population coding of natural scenes in the early visual system. PLoS Biol 6 (12), e324.

Doiron, B., Chacron, M. J., Maler, L., Longtin, A., Bastian, J., jan 2003. Inhibitory feedback required for network oscillatory responses to communication but not prey stimuli. Nature 421, 539–543.

Doiron, B., Lindner, B., Longtin, A., Maler, L., Bastian, J., 2004. Oscillatory activity in electrosensory neurons increases with the spatial correlation of the stochastic input stimulus. Phys. Rev. Lett. 93 (4), 048101.

Engel, A., Kreiter, A.K., Konig, P., Singer, W., 1991. Synchronization of oscillatory neuronal responses between striate and extrastriate visual cortical areas of the cat. Proc. Natl. Acad. Sci. 88, 6048–6052.

Eppler, J. M., Helias, M., Muller, E., Diesmann, M., Gewaltig, M., 2009. Pynest: a convenient interface to the nest simulator. Front. Neuroinform. 2, 12.

Fischer, I., Vicente, R., Buldu, J. M., Peil, M., Mirasso, C. R., Torrent, M. C., Garcia-Ojalvo, J., 2006. Zero-lag long-range synchronization via dynamical relaying. Physical Review Letters 97, 123902.

Fries, P., 2005. A mechanism for cognitive dynamics: neuronal communication through neuronal coherence. Trends in Cognitive Sciences 9, 474–480.

Fries, P., Nikolić, D., Singer, W., 2007. The gamma cycle. Trends Neurosci. 30, 309–316.

Gollo, L. L., Kinouchi, O., Copelli, M., 2009. Active dendrites enhance neu-

ronal dynamic range. PLoS Comput Biol 5 (6), e1000402.
Gray, C. M., König, P., Engel, A. K., Singer, W., 1989. Oscillatory responses in cat visual cortex exhibit inter-columnar synchronization which reflects global stimulus properties. Nature 338, 334–337.
Groh, A., de Kock, C. P. J., Wimmer, V. C., Sakmann, B., Kuner, T., 2008. Driver or coincidence detector: Modal switch of a corticothalamic giant synapse controlled by spontaneous activity and short-term depression. Journal of Neuroscience 8, 9652–9663.
Hayon, G., Abeles, M., Lehmann, D., 2005. A model for representing the dynamics of a system of synfire chains. J. Comp. Neurosci. 18, 41–53.
Huguenard, J. R., McCormick, D. A., 2007. Thalamic synchrony and dynamic regulation of global forebrain oscillations. Trends in Neurosciences 30, 350–356.
Jones, E. G., 1985. The Thalamus. Plenum Press, New York.
Knoblauch, A., Sommer, F. T., 2004. Spike-timing-dependent synaptic plasticity can form "zero lag links" for cortical oscillations. Neurocomputing 58-60, 185–190.
König, P., Engel, A., Singer, W., 1995. Relation between oscillatory activity and long-range synchronization in cat visual cortex. Proc Natl Acad Sci USA 92, 290–294.
Krahe, R., Gabbiani, F., 2004. Burst firing in sensory systems. Nat Rev Neurosci. 5, 13–23.
Marinazzo, D., Kappen, H. J., Gielen, S. C. A. M., 2007. Input-driven oscillations in networks with excitatory and inhibitory neurons with dynamic synapses. Neural Computation 19 (7), 1739–1765.
McAlonan, K., Cavanaugh, J., Wurtz, R. H., 2008. Guarding the gateway to cortex with attention in visual thalamus. Nature 456, 391–394.
McCormick, D., Bal, T., 1994. Sensory gating mechanisms of the thalamus. Current Opinion in Neurobiology 4, 550–556.
Milo, R., Shen-Orr, S., Itzkovitz, S., Kashtan, N., Chklovskii, D., Alon, U., 2002. Simple building blocks of complex networks. Science 298, 824 – 827.
Nikolić, D., 2009. Model this! seven empirical phenomena missing in the models of cortical oscillatory dynamics. In: Proceedings of the International Joint Conference on Neural Networks, IJCNN.
Ringo, J. L., Doty, R. W., Demeter, S., Simard, P. Y., 1994. Time is the essence: A conjecture that hemispheric specialization arises from interhemispheric conduction delay. Cerebral Cortex 4, 331–343.
Rouiller, E. M., Welker, E., 2000. A comparative analysis of the morphology of corticothalamic projections in mammals. Brain Research Bulletin 53, 727–741.
Salami, M., Itami, C., Tsumoto, T., Kimura, F., 2003. Change of conduction velocity by regional myelination yields to constant latency irrespective of distance between thalamus to cortex. Proc. Natl. Acad. Sci. 100, 6174–6179.
Salinas, E., Sejnowski, T., 2001. Correlated neuronal activity and the flow of neuronal information. Nat. Rev. Neurosci. 2, 539–550.

Scheller, B., Daunderer, M., Pipa, G., 2009. General anesthesia increases temporal precision and decreases power of the brainstem auditory-evoked response-related segments of the electroencephalogram. Anesthesiology 111, 340–355.

Shepherd, G. M. (Ed.), 1998. The Synaptic Organization of the Brain. Oxford University Press.

Sherman, S. M., 2001. Tonic and burst firing: dual modes of thalamocortical relay. Trends Neurosci. 24, 122–6.

Sherman, S. M., 2005. Thalamic relays and cortical functioning. Prog Brain Res. 149, 107–26.

Steriade, M., Llinas, R. R., 1988. The functional states of the thalamus and the associated neuronal interplay. Physiological Review 68, 649–742.

Swadlow, H., 2000. Information flow along neocortical axons. In: Miller, R. (Ed.), Time and the Brain. Conceptual Advances in Brain Research. Harwood Academic Publishers, Amsterdam, Ch. 4, pp. 131–155.

Takayanagi, M., Ojima, H., 2006. Microtopography of the dual corticothalamic projections originating from domains along the frequency axis of the cat primary auditory cortex. Neuroscience 142, 769–780.

Tetko, I. V., Villa, A. E. P., 1997. Efficient partition of learning datasets for neural network training. Neural Networks 10, 1361–1374.

Tiesinga, P., Fellows, J., Sejnowski, T., 2008. Regulation of spike timing in visual cortical circuits. Nature Rev. Neuroscience 9, 97–109.

Traub, R. D., Whittington, M. A., Stanford, I. M., Jefferys, J. G. R., 1996. A mechanism for generation of long-range synchronous fast oscillations in the cortex. Nature 383, 621–624.

Uhlhaas, P., Pipa, G., Lima, B., Melloni, L., Neuenschwander, S., Nikolić, D., Singer, W., 2009. Neural synchrony in cortical networks: history, concept and current status. Front. Integr. Neurosci. 3.

Vicente, R., Gollo, L. L., Mirasso, C., Fischer, I., Pipa, G., 2009. Coherent Behavior in Neuronal Networks. Springer New York, Ch. Far in space and yet in synchrony: neuronal mechanisms for zero-lag long-range synchronization, pp. 143–167.

Vicente, R., Gollo, L. L., Mirasso, C. R., Fischer, I., Pipa, G., 2008. Dynamical relaying can yield zero time lag neuronal synchrony despite long conduction delays. Proc. Natl. Acad. Sci. 105, 7157–17162.

Villa, A. E. P., 2002. Cortical modulation of auditory processing in the thalamus. In: Lomber, S. G., Galuske, R. A. W. (Eds.), Virtual lesions: Examining Cortical Function with reversible Deactivation. Oxford University Press, Oxford, UK, Ch. 4, pp. 83–119.

Villa, A. E. P., Bajo, V. M., Vantini, G., 1996. Nerve growth factor (ngf) modulates information processing in the auditory thalamus. Brain Research Bulletin 39, 139–147.

Villa, A. E. P., Rouiller, E. M., Simm, G. M., Zurita, P., de Ribaupierre, Y., de Ribaupierre, F., 1991. Corticofugal modulation of information processing in the auditory thalamus of the cat. Exp. Brain Res. 86, 506–517.

Villa, A. E. P., Tetko, I. V., Dutoit, P., De Ribaupierre, Y., De Ribaupierre, F., 1999a. Corticofugal modulation of functional connectivity within the auditory thalamus of rat. J. Neurosci. Meth. 86, 161–178.

Villa, A. E. P., Tetko, I. V., Hyland, B., A., N., 1999b. Spatiotemporal activity patterns of rat cortical neurons predict responses in a conditioned task. Proc. Natl. Acad. Sci. 96, 1006–1011.

von der Marlsburg, C., 1973. Self-organization of orientation selective cells in the striate cortex. 14:85–100. Kybernetic 14, 85–100.

von Kriegstein, K., Patterson, R. D., Griffiths, T. D., 2008. Task-dependent modulation of medial geniculate body is behaviorally relevant for speech recognition. Curr. Biol. 18, 1855–1859.

Wolfart, J., Debay, D., Masson, G., Destexhe, A., Bal, T., 2005. Synaptic background activity controls spike transfer from thalamus to cortex. Nature Neuroscience 8, 1760–1767.

Yu, X., Xu, X., He, S., He, J., 2009. Change detection by thalamic reticular neurons. Nat Neurosci 12 (9), 1165–1170.